Central European Journal of Energetic Materials
ISSN 1733-7178; e-ISSN 2353-1843
Copyright © 2019 Łukasiewicz Research Network – Institute of Industrial Organic Chemistry, Poland

Cent. Eur. J. Energ. Mater. 2019, *16*(2): 216-227; DOI: 10.22211/cejem/109742
Article is available in PDF-format, in colour, at:
http://www.wydawnictwa.ipo.waw.pl/cejem/Vol-16-Number-2-2019/CEJEM_00944.pdf


Article is available under the Creative Commons Attribution-Noncommercial-NoDerivs 3.0 license CC BY-NC-ND 3.0.

Research paper

Preparation of Insensitive RDX by Suspension Spray Technology and Its Characterization

Xiang Yan,[1] Xiao Dong Li,[1] Peng Zhou,[1] Wei Ji,[2] Xiao Feng Shi [1]
[1] *North University of China, China*
[2] *Southwest University of Science and Technology, China*

Abstract: A new insensitive and high energy explosive based on RDX was prepared by suspension spray technology using Estane 5703 as a binder (e-RDX). Scanning electron microscopy was used to characterize the morphology and particle size of the samples. The composite was analyzed by differential scanning calorimetry and X-ray photoelectron spectroscopy. Its impact sensitivity and detonation velocity were determined. For comparison, raw RDX, refined RDX (r-RDX) and solution spray dried RDX/Estane 5703 (e1-RDX) were also tested using these five methods. The SEM results showed that the e-RDX size was 1-3 μm. e1-RDX exhibited a spherical shape with some defects on the surface. The XPS results indicated that Estane 5703 can be successfully coated onto the surface of e-RDX. Compared to raw RDX, the drop height of r-RDX, e1-RDX and e-RDX was increased, being 16.5 cm, 32.9 cm and 58.4 cm, respectively. The activation energy of e-RDX is lower than that of raw RDX, but a little higher than that of e1-RDX. Compared to raw RDX, the detonation velocity of r-RDX, e1-RDX, w-RDX and e-RDX had decreased, being 110 m·s^{-1}, 710 m·s^{-1}, 410 m·s^{-1} and 210 m·s^{-1}, respectively.

Keywords: RDX, Estane 5703, suspension spray technology, detonation velocity, insensitivity

Nomenclature list

A Pre-exponential factor [s^{-1}]
E Activation energy [J·mol^{-1}]
D Detonation velocity [m·s^{-1}]

H_{50} 50% Explosion probability
M Mass [kg]
R Gas constant, 8.314 J·mol^{-1}·K^{-1}
S Standard deviation
T_{pi} Temperature of the exothermic peak at β_i heating rate, [K]
β_i Heating rate [K·min^{-1}]
Φ Diameter [mm]

1 Introduction

1,3,5-Trinitro-1,3,5-triazinane (RDX) is a high explosive (HE) and is widely used in weapons. The application of RDX is under restriction because of its high sensitivity. Various binders have therefore been added to RDX-based explosives to reduce their sensitivity [1-5]. Estane is a widely used hydrocarbon polymer in the explosive industry due to its excellent performance [6-12]. Plastic bonded explosives (PBXs) that are coated with Estane display many advantages, such as excellent toughness and are shatterproof. Alternatively, changing the crystal size and morphology has been studied as a means to reduce the sensitivity of RDX. Micron- and nanometer-sized RDX particles have been prepared by various techniques [13-15]. These RDX particles retain their energy but are less sensitive. Spherical and cubic explosive particles have been prepared to reduce RDX sensitivity [16-18].

Spray drying is a single step synthesis technology that can be used to prepare ultrafine and spherical composite particles. It has been employed in the fabrication of energetic materials. Qiu [19] produced RDX-based composite explosives by using the suspension spray technology. By observing the cross-section of the crystals of the explosives, Qiu found that the size of the crystals in the explosives decreases radially from the centers of the crystals to their surfaces. It is also found that the size of the liquid droplets has a significant effect on both the size and size distribution of the RDX crystals. Alhalaweh [20] found that pure cocrystals can be generated simply by spray drying and the formation of cocrystals under incongruent saturation conditions undermines the importance of thermodynamic phenomena. Shi [21] prepared HMX/Estane nanocomposite particles that were 1-8 μm spheres. Compared to raw RDX, the thermal stability of HMX/Estane is better and the impact sensitivity is lower. Wang [22] prepared CL-20/TNT explosive cocrystals with particle sizes in the range 1-10 μm. In the DSC test, there were two peak temperatures of exothermic decomposition. The impact sensitivity (H_{50}) of CL-20/TNT explosive cocrystals was 36.2 cm higher than that of raw CL-20.

Copyright © 2019 Łukasiewicz Research Network – Institute of Industrial Organic Chemistry, Poland

However, water suspension technology is another method for coating explosives, but the coated particles are not of uniform size and uneven coating readily occurs. Because of this concern, the idea of suspension spray drying technology was used in this paper, which can make particles that are evenly coated but can also create coated particles that are spherical. As the adhesion agent of explosives, Estane exhibits very good mechanical properties, such as viscoelasticity, static stretch and compression. When Estane is coated on the surface of RDX particles, it has good adhesive properties, good covering ability and compatibility, and reduces the sensitivity of the explosive. In the present work, using Estane 5703 as the binder, RDX-based spheres were prepared by suspension spray technology and solution spray drying technology. Furthermore, the properties of the RDX-based products were characterized and analyzed in detail.

2 Experimental

2.1 Materials

RDX was produced by Gansu YingGuang Chemical Industry Group Co., Ltd.; Estane was provided from Dongguan XiangLin Plastic Co., Ltd.; acetone, 1,2-dichloroethane and dimethyl sulfoxide (DMSO) were purchased from Tianjin TianDa Chemicals Co., Ltd.

2.2 Preparation of RDX based spheres

2.2.1 The suspension spray drying process

The experimental equipment is shown in Figure 1. The experimental procedures were as follows: Firstly, raw RDX (5 g) was dissolved in DMSO (20 mL) to give a solution with a concentration of 0.25 g·mL^{-1}. The solution was injected into a beaker containing an anti-solvent (purified water) *via* a nozzle. Refined RDX (r-RDX) was obtained after filtration and drying. Secondly, the binder, Estane 5703, was dissolved in 1,2-dichloroethane to form a solution and the refined RDX power was mixed into the 1,2-dichloroethane solution to form a suspension using sonication and stirring. Thirdly, the suspension was spray dried using a Spray Dryer B-290 (BUCHI Labortechnik AG) and the product (e-RDX) was obtained. Finally, the product was vacuum dried in an oven for 1 day at 30 °C. The experimental conditions were as follows: a double-fluid spray nozzle with inner diameter 0.07 mm was used; experimental proportions:

– $M_{(\text{refined RDX})}$:$M_{(\text{Estane 5703})}$ = 95:5,
– $M_{(\text{1,2-dichloroethane})}$:$M_{(\text{refined RDX})}$ = 98:2.

Copyright © 2019 Łukasiewicz Research Network – Institute of Industrial Organic Chemistry, Poland

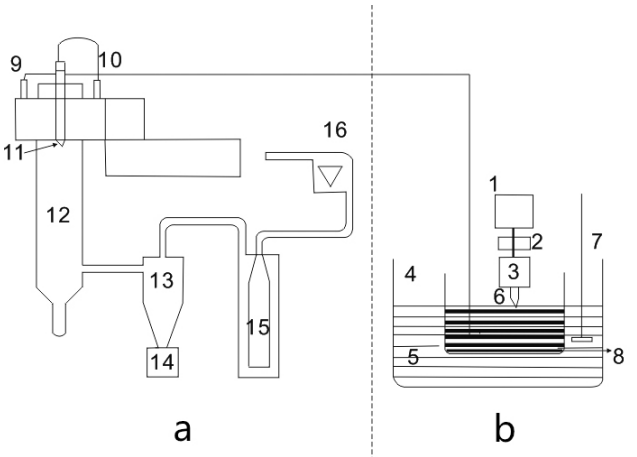

Figure 1. Experimental apparatus for the suspension spray process: 1 – controlled-volume pump; 2 – valve; 3 – RDX solution; 4 – ultrasonic apparatus; 5 – water; 6 – homemade nozzle; 7 – stirrer; 8 – *n*-heptane; 9 – compressed air connection; 10 – cooling water connection; 11 – double-fluid spray nozzle; 12 – spray cylinder; 13 – cyclone separator; 14 – product collection container; 15 – outlet filter; 16 – air purge unit

2.2.2 The solution spray drying process

The experimental setup is shown in Figure 1(a). The solvent in the solution shown in Figure 1(b) is acetone, and the solute consists of raw RDX and Estane 5703; the ratio of $M_{(1,2\text{-dichloroethane})}$ to $M_{(\text{refined RDX})}$ is 95:5. The product (e1-RDX) was obtained from the product collection container.

In this paper, r-RDX represents the fine RDX particles without Estane, e-RDX designates the particles coated with Estane in a solvent which cannot dissolve RDX except Estane, while e1-RDX is the composite made from a mixed solution of RDX and Estane.

2.3 Characterization

The morphology and size of the products were studied using a Hitachi S-4800 scanning electron microscope (SEM) (Hitachi Ltd., Japan). The accelerating voltage was 1.0 kV. Differential scanning calorimetry (DSC) experiments were conducted in an N_2 atmosphere using a Setaram DSC131 instrument (Setaram Instrumentation Co., France) and an aluminum crucible with a hole in the cap. The test conditions were: sample mass, 0.7 mg; N_2 flow rate, 15 mL·min^{-1} and sample heating rates, 20 K·min^{-1}, 10 K·min^{-1} and 5 K·min^{-1}.

Copyright © 2019 Łukasiewicz Research Network – Institute of Industrial Organic Chemistry, Poland

Vacuum stability was tested with a Stabil 21 dynamic vacuum stability apparatus. The impact sensitivity of the products was tested at room temperature using an ERL type 12 drop hammer apparatus with a sample mass of 35 ±1 mg and a drop weight of 5 ±0.002 kg. Four groups of each sample and 25 of the same sample from each group were tested. The results were generated in terms of the critical drop-height H_{50} and the standard deviation S. An Axis Ultra Imaging Photoelectron Spectrometer (Kratos Analytical Ltd., England) was used to contrast the surface elements of the products by X-ray photoelectron spectroscopy (XPS). The detonation velocity was measured with a TSN632M type 32 channel detonation velocity meter. The samples were pressed into explosive pellets with a size of 10 mm Φ × 10 mm at 90% of the theoretical maximum density (TMD).

3 Results and Discussion

3.1 SEM Characterization

Figure 2(a) shows that the particle size of raw RDX ranged from 50 μm to 100 μm, and had a chunky appearance. The refined RDX was 1-3 μm in size [see Figure 2(b)]. The samples sprayed with a mixed solution are spheres with diameters of 2 μm to 10 μm, but some holes are observed on the spherical surfaces, as seen in Figure 2(c). This is because the hot N_2 gas contacts with the surface of the mixed solution and transfers heat from the outside of the solution to its inside which leads to a temperature difference between the outside and inside. The explosive and binder were precipitated to form the outermost shell on the droplet surface. With the evaporation of the solvent, the internal pressure increased and the surface formed a closed spherical shell. However, some solvent trapped inside the shell broke through the shell to form holes on the surface in the extrusion process. From Figure 2(d), the particles prepared by the suspension spray drying method were solid ellipsoids with good structure and particle size of 1-3 μm. A white coating layer could be readily observed on the surface of the e-RDX granules, the particle size was uniform, the surface smooth with no defects. The coating process was a physical process. This process could be explained by adsorption theory. When Estane was dissolved in the solvent and was contacted with RDX, the Estane gradually adsorbed the RDX crystals due to intermolecular forces (the distance between the molecules was less than 0.5 nm).

Copyright © 2019 Łukasiewicz Research Network – Institute of Industrial Organic Chemistry, Poland

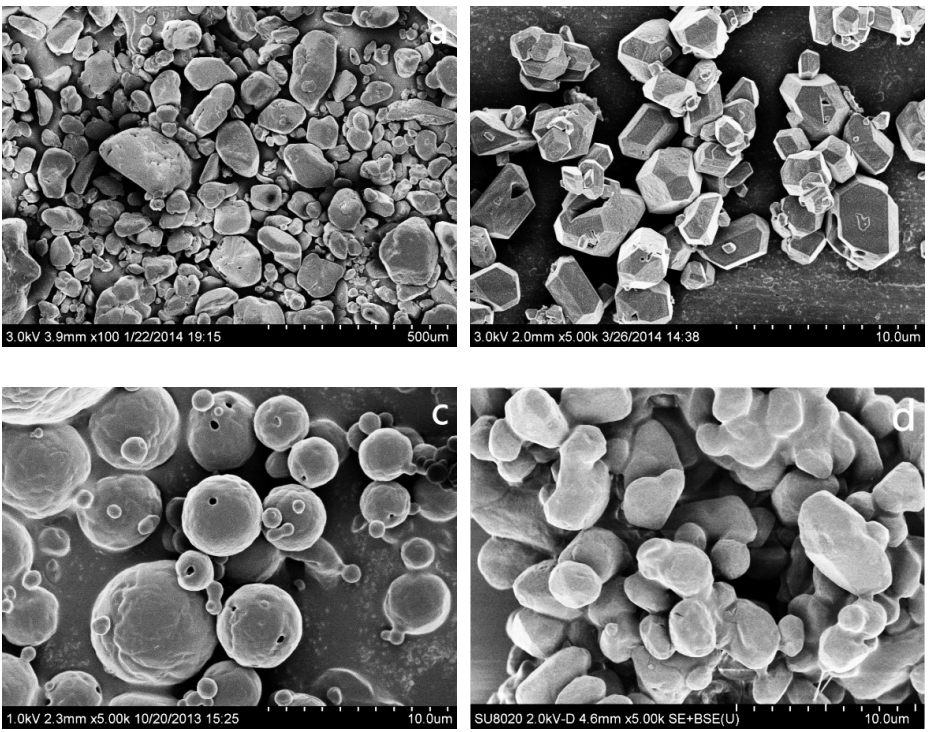

Figure 2. SEM images of (a) raw RDX, (b) r-RDX, (c) e1-RDX and (d) e-RDX

3.2 Thermal decomposition characteristics

Figure 3 shows the DSC curves of raw RDX, r-RDX, e1-RDX and e-RDX at heating rates of 20 K·min^{-1}, 10 K·min^{-1} and 5 K·min^{-1}. There was an endothermic peak at 202-204 °C in all of the DSC curves in Figure 3. These curves showed that the RDX began to melt at 202-204 °C. For the same sample, the exothermic peak temperature was lower at slower heating rates. The thermal decomposition kinetic parameters of raw RDX, r-RDX, e1-RDX and e-RDX can be calculated by the Kissinger method (Equation 1) [23]. Thermal stability refers to the high temperature-resistance property of materials and their ability to maintain stable properties with heating. It can be expressed using the self-ignition temperature (T_b), which can be estimated from Equations 4 [24] and 5 [25].

Copyright © 2019 Łukasiewicz Research Network – Institute of Industrial Organic Chemistry, Poland

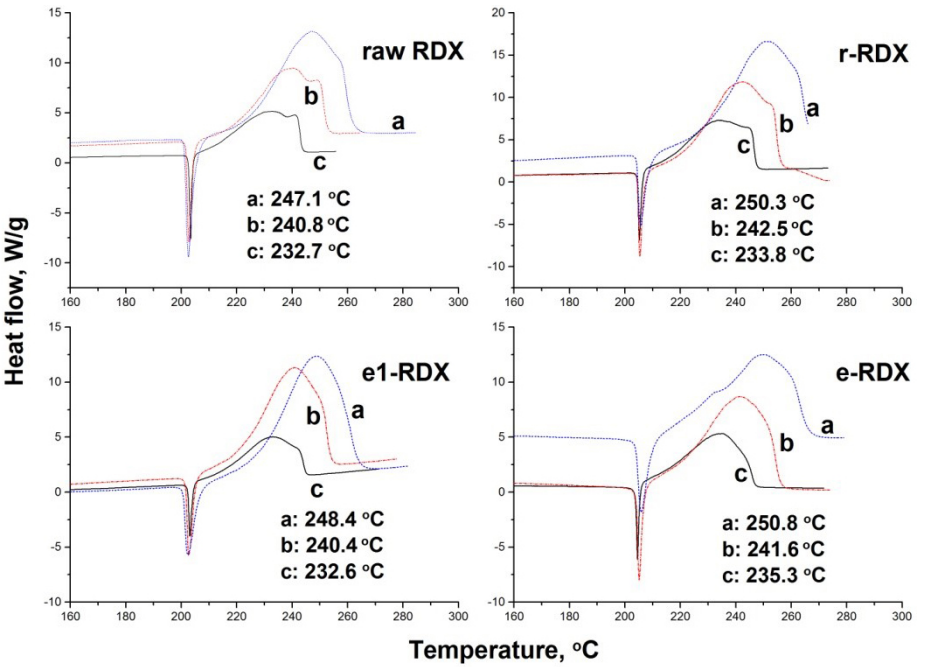

Figure 3. DSC curves of raw RDX, r-RDX, e1-RDX and e-RDX at heating rates of (a) 20 K·min^{-1}, (b) 10 K·min^{-1}, and (c) 5 K·min^{-1}

$$\ln\frac{\beta_i}{T_{pi}^2} = \ln\frac{AR}{E} - \frac{E}{RT_{pi}} \tag{1}$$

$$A = \frac{E_a \beta_i}{RT_p^{\,2}} \exp\left(\frac{E_a}{RT}\right) \tag{2}$$

$$k = A\exp\left(-\frac{E_a}{RT}\right) \tag{3}$$

$$T_{pi} = T_{p0} + b\beta_i + c\beta_i^2 \tag{4}$$

$$T_b = \frac{E_a - \sqrt{E_a^2 - 4RE_aT_{p0}}}{2R} \tag{5}$$

Based on these data, the activation energy (E), frequency factor (A), peak temperature (T_p) and critical explosion temperature (T_b) of the RDX-based samples can be calculated and are shown in Table 1. The activation energy of r-RDX is lower than that of raw RDX because of its smaller

Copyright © 2019 Łukasiewicz Research Network – Institute of Industrial Organic Chemistry, Poland

particle size, making heat dissipation easier, but the specific surface area of r-RDX had increased, leading to an apparent decrease in activation energy. However, the activation energies of e-RDX and e1-RDX were different to that of r-RDX because of the Estane in their explosive formulas. The T_b results indicated that the thermal stability of e-RDX was superior to that of raw RDX, r-RDX and e1-RDX. RDX and Estane 5703 exhibited good compatibility.

Table 1. Thermal explosion and critical temperature data for RDX-based energetic materials

Sample	E_a [kJ·mol^{-1}]	lg$A$ [s^{-1}]	T_p [°C]	T_b [°C]
raw RDX	201.3	20.4	221.3	231.9
r-RDX	205.2	21.3	210.6	232.5
e1-RDX	175.8	17.7	222.1	233.9
e-RDX	190.5	19.1	228.2	239.4

3.3 Impact Sensitivity

From Table 2, the drop height of the RDX-based samples from highest to lowest were: e-RDX > e1-RDX > r-RDX > raw RDX. These results proved that the impact sensitivity of e-RDX is lower than that of e1-RDX, r-RDX and raw RDX. The influence of mechanical stimulation on the sensitivity of RDX samples could be analyzed as follows:

(1) Compared to raw RDX, the particle size of r-RDX is smaller, crystal defects are reduced and the particle surfaces are smooth. It is not easy to form local hot spots under mechanical stimuli, leading to reduced sample sensitivity.

(2) The Estane in e-RDX and e1-RDX could reduce the energy and mechanical sensitivity of the particles with the same packing density. Meanwhile, the binder coated onto the RDX surface could prevent friction between the explosive particles and serve as a shock absorber or diverter under mechanical stimuli, thereby leading to a reduction in the probability of hot spot formation.

(3) The e-RDX consists of solid particles, while e1-RDX exhibits some holes on its surface and these holes can increase the mechanical sensitivity of the explosive. The micro-particle size, crack-free surface and the addition of the binder can also reduce the mechanical sensitivity. The results show that e-RDX possesses an outstanding insensitive character.

Copyright © 2019 Łukasiewicz Research Network – Institute of Industrial Organic Chemistry, Poland

Table 2. Impact sensitivity of RDX-based samples

Sample	Impact sensitivity, H_{50} [cm] and (S)				
	Experiment				Average
	1	2	3	4	
raw RDX	20.5 (0.07)	21.6 (0.06)	22.6 (0.05)	20.1 (0.08)	18.4
r-RDX	35.5 (0.07)	33.7 (0.06)	34.3 (0.06)	35.9 (0.05)	34.9
e1-RDX	50.6 (0.04)	52.7 (0.08)	51.3 (0.06)	50.4 (0.03)	51.3
e-RDX	76.8 (0.06)	77.8 (0.05)	75.3 (0.07)	77.4 (0.08)	76.8

3.4 X-ray photoelectron spectroscopic characterization

The distribution of the surface elements for RDX-based samples were characterized by XPS. The results are listed in Table 3. As is shown in Table 3, the "N" content of an Estane 5703 surface is very low, but the "C" content is higher. The "N", "O" and "C" contents on the surface of raw RDX are relatively uniform. Compared to raw RDX, the element distribution on r-RDX has changed little. The "N" contents on the surfaces of e1-RDX and e-RDX are reduced by 16.76% and 27.19%, respectively; while the "C" content are increased by 21.65% and 32.23% accordingly. Therefore, the coating effect of e-RDX is better than that of e1-RDX.

Table 3. Distribution of surface elements on RDX-based samples

Sample	Surface element [%]		
	O 1s	N 1s	C 1s
Estane 5703	29.80	2.95	67.35
raw RDX	33.20	34.82	32.16
r-RDX	33.00	35.82	31.18
e1-RDX	28.13	18.06	53.81
e-RDX	27.98	7.63	64.39

3.5 Detonation velocity

In order to compare the effects of the different preparative processes on the detonation velocity of RDX-based explosives, w-RDX composite explosives, experimental formulations: $M_{(\text{refined RDX})}$:$M_{(\text{Estane 5703})}$ = 95:5, were prepared by the water-slurry coating method [26, 27]. The detonation velocity of the RDX-based samples was tested and the results are listed in Table 4.

As shown in Table 4, the reduction of the detonation velocity of RDX after the refining processing is minor. The detonation velocities of e1-RDX, w-RDX and e-RDX were reduced by 710 m·s^{-1}, 410 m·s^{-1} and 210 m·s^{-1}, respectively, compared with raw RDX. This demonstrates that the detonation velocity

Copyright © 2019 Łukasiewicz Research Network – Institute of Industrial Organic Chemistry, Poland

of RDX-based samples prepared by suspension spray technology is higher than that of products coated by other technologies.

Table 4. The values of detonation velocity for RDX-based samples

Sample	D [m·s^{-1}]	ΔD [m·s^{-1}]
raw RDX	8310	29
r-RDX	8200	50
e1-RDX	7600	30
e-RDX	8100	34
w-RDX	7900	32

4 Conclusions

RDX-based products, which were coated with Estane 5703, were successfully prepared by suspension spray technology (e-RDX) and solution spray drying technology (e1-RDX). The e-RDX was 1-3 μm in size and was ellipsoid in shape. e1-RDX exhibited a spherical shape, but had some defects on the surface. The proportions of elements on the surface of e-RDX was very different to that of raw RDX. This is because of the Estane 5703 coating on the surface of the RDX, which changes the proportion of the surface elements originally present. The activation energy of e-RDX is lower than that of raw RDX, but a little higher than that of e1-RDX. The impact sensitivities of e-RDX and e1-RDX were lower than that of the raw RDX as indicated by a greater drop height. The detonation velocity of e-RDX was higher than that of e1-RDX. These combined properties suggest that e-RDX energetic spheres are an insensitive, but highly energetic explosive, with great potential.

References

[1] Jangid, S.K.; Singh, M.K.; Solanki, V.J.; Talawar, M.B.; Nath, T. 1,3,5-Trinitroperhydro-1,3,5-triazine (RDX)-Based Sheet Explosive Formulation with a Hybrid Binder System. *Propellants Explos. Pyrotech.* **2016**, *41*(2): 377-382.

[2] Kaur, J.; Arya, V.P.; Kaur G.; Lata P. Evaluation of the Thermo-mechanical and Explosive Properties of Bimodal and Hybrid Polymer Bonded Explosive (PBX) Compositions Based on HNS and HMX. *Cent. Eur. J. Energ. Mater.* **2013**, *10*(3): 371-391.

[3] Elbeih, A.; Mohamed, M.M.; Wafy, T. Sensitivity and Detonation Characteristics of Selected Nitramines Bonded by Sylgard Binder. *Propellants Explos. Pyrotech.*

Copyright © 2019 Łukasiewicz Research Network – Institute of Industrial Organic Chemistry, Poland

2016, *41*(6): 1-7.

[4] Elbeih, A.; Pachman, J.; Zeman, S.; Vávra, P.; Trzciński, W.A.; Akštein, Z. Detonation Characteristics of Plastic Explosives Based on Attractive Nitramines with Polyisobutylene and Poly(methyl methacrylate) Binders. *J. Energ. Mater.* **2012**, *30*(4): 358-371.

[5] Burnham, A.K.; Weese, R.K. Kinetics of Thermal Degradation of Explosive Binders Viton A, Estane, and Kel-F. *Thermochim. Acta* **2005**, *426*(1-2): 85-92.

[6] Barua, A.; Horie, Y.; Zhou, M. Energy Localization in HMX-Estane Polymer-bonded Explosives during Impact Loading. *J. Appl. Phys.* **2012**, *111*(5): 399-586.

[7] Jia, X.L.; Zhang, Y.P.; Hou, C.H.; Wang, J.Y.; Ren, L.P. Preparation and Characterization of Polymer Bonded Explosive of HMX/TATB at Different Ratios. (in Chinese) *Zhongbei Daxue Xuebao* **2017**, *38*(3): 360-363 and 372.

[8] Barua, A.; Zhou, M. Computational Analysis of Temperature Rises in Microstructures of HMX-Estane PBXs. *Comput. Mech.* **2013**, *52*(1): 151-159.

[9] Singh, G.; Prem, F.S.; Soni, P. Studies on Energetic Compounds, Part 28: Thermolysis of HMX and Its Plastic Bonded Explosives Containing Estane. *Thermochim. Acta* **2003**, *399*(1): 153-165.

[10] Xiao, J.J.; Huang, H.; Li, J.S.; Zhang, H.; Zhu, W.; Xiao, H.M. Computation of Interface Interactions and Mechanical Properties of HMX-based PBX with Estane 5703 from Atomic Simulation. *J. Mater. Sci.* **2008**, *43*(17): 5685-5691.

[11] Kim, H.; Lagutcheva, A.; Dlott, D.D. Surface and Interface Spectroscopy of High Explosives and Binders: HMX and Estane. *Propellants Explos. Pyrotech.* **2006**, *31*(2): 116-123.

[12] Barua, A.; Horie, Y.; Zhou, M. Microstructural Level Response of HMX–Estane Polymer-bonded Explosive under Effects of Transient Stress Waves. *P. Roy. Soc. A-Math. Phy.* **2012**, *468*(2147): 3725-3744.

[13] Wang, Y.; Jiang, W.; Song, X.L.; Deng, G.D.; Li, F.S. Insensitive HMX (Octahydro-1,3,5,7-tetranitro-1,3,5,7-tetrazocine) Nanocrystals Fabricated by High-yield, Low-cost Mechanical Milling. *Cent. Eur. J. Energ. Mater.* **2013**, *10*(2): 277-287.

[14] Zohari, N.; Keshavarz, M.H.; Seyedsadjadi, S.A. The Advantages and Shortcomings of Using Nano-sized Energetic Materials. *Cent. Eur. J. Energ. Mater.* **2013**, *10*(1): 135-147.

[15] Pichot, V.; Seve, A.; Berthe, J.E.; Schnell, F.; Spitzer, D. Study of the Elaboration of HMX and HMX Composites by the Spray Flash Evaporation Process. *Propellants Explos. Pyrotech.* **2017**, *42*(12): 1-7.

[16] Song, X.L.; Wang, Y.; An, C.W.; Guo, X.D. Dependence of Particle Morphology and Size on the Mechanical Sensitivity and Thermal Stability of Octahydro-1,3,5,7-tetranitro-1,3,5,7-tetrazocine. *J. Hazard. Mater.* **2008**, *159*(2): 222-229.

[17] Kim, J.W.; Shin, M.S.; Kim, J.K.; Kim, H.S.; Koo, K.K. Evaporation Crystallization of RDX by Ultrasonic Spray. *Ind. Eng. Chem. Res.* **2011**, *50*(21): 12186-12193.

[18] Vijayalakshmi, R.; Radhakrishnan, S.; Rajendra, P.S.; Girish, G.M.; Arun, S.K. Particle Size Management Studies on Spherical 3-Nitro-1,2,4-triazol-5-one. *Part. Part. Syst. Char.* **2012**, *28*(3-4): 57-63.

Copyright © 2019 Łukasiewicz Research Network – Institute of Industrial Organic Chemistry, Poland

[19] Qiu, H.; Stepanov, V.; Stasio, A.R.D; Surapaneni, A.; Lee, W.Y. Investigation of the Crystallization of RDX during Spray Drying. *Powder Technol.* **2015**, *274*: 333-337.
[20] Alhalaweh, A.; Velaga, S.P. Formation of Cocrystals from Stoichiometric Solutions of Incongruently Saturating Systems by Spray Drying. *Cryst. Growth Des*. **2010**, *10*(8): 3302-3305.
[21] Shi, X.; Wang, J.; Li, X.; An, C. Preparation and Characterization of HMX/Estane Nanocomposites. *Cent. Eur. J. Energ. Mater.* **2014**, *11*(3):433-442.
[22] Wang, J.Y.; Li, H.Q.; An, C.W.; Guo, W.J. Preparation and Characterization of Ultrafine CL-20/TNT Cocrystal Explosive by Spray Drying Method. (in Chinese) *Chin. J. Energ. Mater.* (*Hanneng Cailiao)* **2015**, *11*:1103-1106.
[23] Kissinger, H.E. Reaction Kinetics in Differential Thermal Analysis. *Anal. Chem.* **1957**, *29*(11): 1702-1706.
[24] Zhang, T.L.; Hu, R.Z.; Xie, Y.; Li, F.P. The Estimation of Critical Temperatures of Thermal Explosion for Energetic Materials Using Non-isothermal DSC. *Thermochim. Acta* **1994**, *244*: 171-176.
[25] Sovizi, M.R.; Hajimirsadeghi, S.S.; Naderizadeh, B. Effect of Particle Size on Thermal Decomposition of Nitrocellulose. *J. Hazard. Mater.* **2009**, *168*(2-3): 1134-1139.
[26] Lei, Y.C.; Wang, J.Y. Study on Slurry Coating Technique for Preparation of TATB/HMX Based PBX. (in Chinese) *Chin. J. Explos. Propellants (Huozhayao Xuebao)* **2015**, *38*(4): 59-62.
[27] Shen, J.T.; Xu, W.Z.; Wang, J.Y. Xing, J.T. Study on the Reduced Sensitivity of HMX Coated with ACM. (in Chinese) *Initiators Pyrotech.* **2016**, *5*: 50-53.

Received: June 8, 2018
Revised: May 17, 2019
First published online: June 27, 2019

Copyright © 2019 Łukasiewicz Research Network – Institute of Industrial Organic Chemistry, Poland